Investigation of the Pressure Drop Across Packed Beds of Spherical Beads: Comparison of Empirical Models With Pore-Level Computational Fluid Dynamics Simulations

A. J. Otaru
Gas Turbine and Transmissions Research Centre,
Faculty of Engineering,
The University of Nottingham,
Nottingham NG7 2RD, UK

A. R. Kennedy
Department of Engineering,
Lancaster University,
Lancaster LA1 4YW, UK

This study uses novel methods, combining discrete element method (DEM) simulations for packing and computational fluid dynamics (CFD) modeling of fluid flow, to simulate the pressure drop across rigid, randomly packed beds of spheres ranging from 1 to 3 mm in diameter, with porosities between 0.34 and 0.45. This modeling approach enables the combined effect of void fraction and particle size to be studied in more depth than that has been previously possible and is used to give insight into the ability of the well-established Ergun equation to predict the pressure drop behavior. The resulting predictions for pressure drop as a function of superficial velocity were processed to yield coefficients α and β in the Ergun equation and were found to be in keeping with equivalent data in the literature. Although the scatter in α with structural variations was very small, the scatter in β was large (±20%), leading to inaccuracies when used to predict pressure drop data at velocities beyond the Darcy regime. Evaluation of the packed particle structures showed that regions of poor packing, in samples with high porosity and large particle sizes, lead to lower β values. The findings bring strong support to the belief that a generalized model, such as that by Ergun, cannot yield a unique value for β, even for identical spheres. [DOI: 10.1115/1.4042957]

Keywords: computational fluid dynamics, porous media, permeability

1 Background

The flow of fluids through porous media is of great interest to many fields. These include water flow through rocks, petroleum recovery processes, sound absorption, and metallurgical processing. The specific case of fluid flow through packed beds of near-spherical particles and the ability to predict and model flow characteristics, such as pressure drop, in such structures is vital to aid the design of efficient chemical reactors, adsorption columns, heat exchangers, and separators.

The pressure-drop-flow velocity relationship for very slow fluid flow through a porous structure can be described by the Hazen–Darcy equation

$$\frac{\Delta P}{L} = \frac{\mu}{k} v \tag{1}$$

where ΔP is the pressure difference across the length of the porous material in the flow direction (Pa), L is the sample thickness in the same direction (m), k is the permeability (m^2), μ is the fluid viscosity (Pa·s), and v is the Darcian velocity, the volumetric flow rate divided by the cross-sectional flow area ($m\ s^{-1}$). For flow behavior obeying this case, the fluid is said to be flowing in the Darcy regime. The Blake–Kozeny equation, shown in Eq. (2) [1], can be used to estimate the permeability, k, of a packed bed of spheres with diameter, d_s, as a function of the porosity or void fraction, ε, and the Blake–Kozeny constant, B_K, which, for spheres, is 36 times the Kozeny constant, K [2]

$$k = \frac{d_s^2}{B_K}\left(\frac{\varepsilon^3}{(1-\varepsilon)^2}\right) \tag{2}$$

The complex and tortuous flow paths in porous media make the Kozeny constant, K, difficult to determine. A K value of 5.0 proposed by Kozeny [2] is universally untrue and K values ranging from 4.5 to 5.1 have been proposed for liquid flow in randomly packed columns and fluidized beds [3]. For gas flow measurement across porous media, Carman [4] proposed an average K value of 4.8 for void fractions ranging from 0.26 to 0.48.

As the fluid velocity increases, the Hazen–Darcy equation fails to describe the pressure-drop behavior [4–6]. A quadratic term, referred to as the Forchheimer or the form drag term, is added to Eq. (1) to capture the effect of the force exerted by any solid surface on the flowing fluid and its resultant effect on the pressure drop. This yields Eq. (3), which is known as the Hazen–Dupuit–Darcy or Forchheimer equation

$$\frac{\Delta P}{L} = \frac{\mu}{k} v + C\rho v^2 \tag{3}$$

where ρ is the fluid density ($kg\ m^{-3}$) and C is the form drag coefficient (m^{-1}). For typical fluid velocities and pore size ranges used in engineering flow systems, the Forchheimer equation most accurately describes such unidirectional fluid flow.

The Ergun relationship has also been adopted by researchers to describe the pressure drop across porous materials [1–4,7,8]; its

Contributed by the Fluids Engineering Division of ASME for publication in the Journal of Fluids Engineering. Manuscript received September 14, 2018; final manuscript received February 14, 2019; published online April 8, 2019. Assoc. Editor: Ning Zhang.

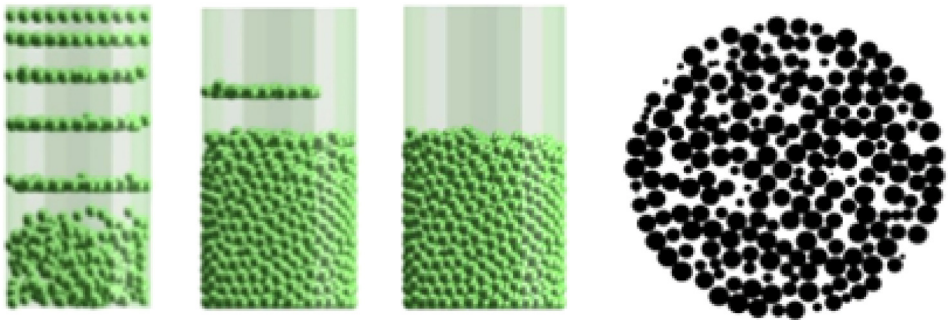

Fig. 1 Discrete element method simulation (left) of the filling of a 35 mm diameter vessel with monosized particles [20], and (right) a horizontal slice through the packed bed

form is similar to the Forchheimer equation and was originally developed for packed columns of spherical particles [9]. The Ergun equation is presented in Eq. (4) where α and β are empirical constants (originally determined by experimentation to be 150 and 1.75) [10]. By comparing Eqs. (3) and (4), the permeability and form drag coefficient can be expressed by Eqs. (5) and (6). For low flow velocities, the right-hand term in Eq. (4) becomes negligible and the similarity to the Darcy and Blake–Kozeny equations is clear, with α being equivalent to B_K. For K values between 4.5 and 5.1, the viscous-related Ergun coefficient (α) is expected to be in the range of 162–184

$$\frac{\Delta P}{L} = \alpha \frac{(1-\varepsilon)^2 \mu}{\varepsilon^3 {d_s}^2} v + \beta \frac{(1-\varepsilon)\rho}{\varepsilon^3 d_s} v^2 \tag{4}$$

where

$$\frac{1}{k} = \alpha \frac{(1-\varepsilon)^2}{\varepsilon^3 {d_s}^2} \tag{5}$$

and

$$C = \beta \frac{(1-\varepsilon)}{\varepsilon^3 d_s} \tag{6}$$

Although Ergun [3] proposed α and β values of 150 and 1.75, successive researchers have proposed a much broader range of values for these constants, due to variations in particle sphericity and roughness [8,9,11] and the structural morphology of the different packed beds investigated. Although, even for spherical particles, α and β values in the range of 160–180 and 1.8–4.36, respectively, have been measured [11–17], there is little understanding, as to the direct influence of structural parameters on these variations.

Efforts have been made to model flow through packed beds of spheres using computational fluid dynamics (CFD), as overviewed in Refs. [18] and [19]. The approaches taken tend to split into those, which either aim to simulate the entire bed (regular or random [20] packing), the size for which is limited by computational power, or those that use a periodic cell approach where each particle is assumed to have a region of influence around it [19]. Some of these studies have used CFD simulations to estimate the Ergun coefficients for packed beds of spheres, yielding $\alpha = 175$ [21] and $\alpha = 182$ and $\beta = 1.75$ [19].

This paper models flow through rigidly packed sphere structures using a novel approach. First, the discrete element method (DEM) is used to simulate packing of monosized spheres in a vessel, based on a methodology described in Ref. [22]. Fluid flow through a subelement at the center of this structure is then modeled using CFD. This yields a pore-level representation of the packed bed structure [23] that is intermediate between more traditional unit cell and full-scale modeling approaches. Unlike regular packing models or sequential packing schemes [21], the packing density in these novel DEM-derived structures can be varied incrementally by varying the interparticle friction [22,24]. This approach has been shown to be a robust method for generating realistic porous structures by replication of spherical particles (the inverse of this structure—where the spheres become the pores [23]) and then modeling airflow [25] and sound absorption [26] in them. Processing and analysis of the data and separation of the relevant flow regimes enable abstraction of key parameters in Eqs. (1)–(6). In this way, the appropriateness of simple empirical models and the universality of the constants used in the Blake–Kozeny and Ergun models can be rigorously tested for a series of controlled test parameters.

2 Modeling Approach

The DEM was used to simulate the packing of spheres in a cylindrical vessel, a schematic of which is shown in Fig. 1. Further details of the DEM approach used are published in Refs. [22] and [24]. Unlike in many other studies, in this work, the packing density was controlled by varying the value for the interparticle friction. Particle sizes and positions for the settled, rigidly packed structures were exported to MATLAB™, in which code was written to create serial two-dimenisional (2D) sections in the Z height, at prescribed intervals. A two-dimensional MATLAB™ generated image slice of the packed spheres (2 mm in diameter with an original pixel size of 21 μm) is presented in Fig. 1 (right). Image stacks were imported into the ScanIP module of SIMPLEWARE™, where the 2D images were restored to a three dimensional (3D) volume. Accurate preservation of the particle shape and fluid volume was achieved by optimizing the smart mask smoothing process within this software. A representative volume element (RVE) was determined by measuring the volume fraction of particles in a unit cell as a function of test volume size. The RVE was selected as the smallest volume for which the particle volume fraction was within $\pm 2\%$ of the bulk value. This was achieved for cubic RVEs with dimensions that were three times the particle diameter. RVEs for 2 mm diameter packed sphere structures with different void contents are presented in Fig. 2.

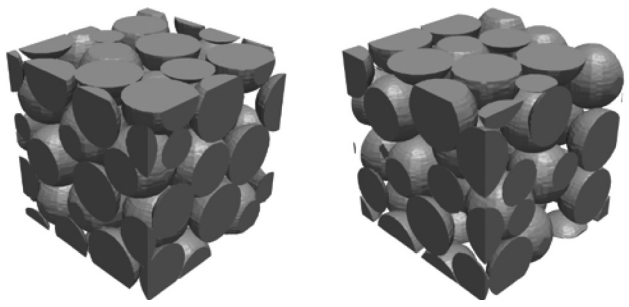

Fig. 2 RVEs for packed beds of 2.0 mm diameter spheres with void fractions of (left) 0.34 and (right) 0.43

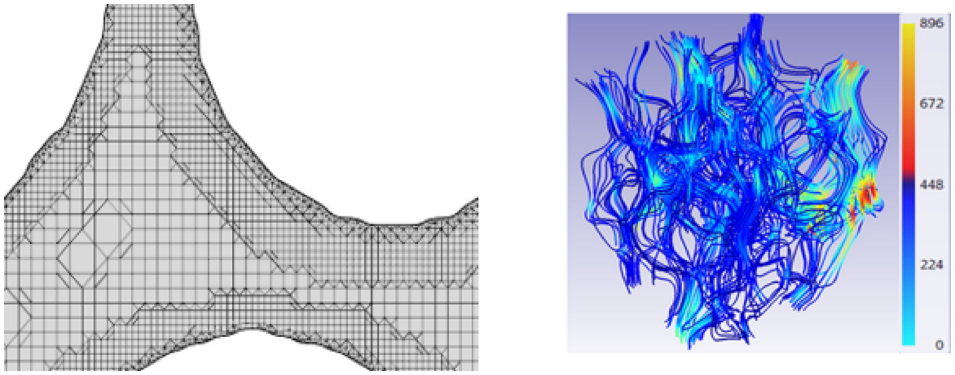

Fig. 3 A 2D (left) of the HQTM mesh structure and (right) a 3D velocity streamline plot (vertical axis units in mm s^{-1})

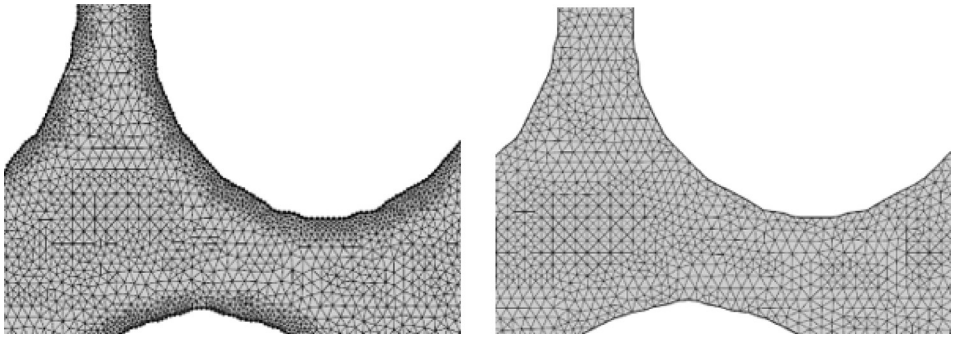

Fig. 4 Two-dimensional images of LTM structures having equal maximum edge length (3× the voxel dimension) and minimum edge of (left) 1× and (right) 2.5× the voxel dimension

A high density hexahedral/quadratic tetrahedral mesh (HQTM also known as finite element (FE)-Grid in SIMPLEWARE) was used as a benchmark for the modeling process. This mesh type creates an RVE with over 25×10^6 cells. Figure 3 (left) shows a 2D section of the FE grid (HQTM) meshed structure, showing a hexahedral mesh in the center of the fluid domain and a tetrahedral mesh on the re-entrant edges. The SIMPLEWARE +FLOW module was used to solve the Navier–Stokes equation, under Darcy flow conditions (it can only solve for Darcy-type flow), to determine the permeability in the height, Z, direction (that which was parallel to the gravity vector during packing). Figure 3 (right) presents a typical three-dimensional fluid phase velocity streamline plot obtained using the +FLOW solver.

The highly dense HQTM mesh structure is computationally expensive to solve in CFD software such as COMSOL™ and the use of a linear tetrahedral mesh (LTM) offers a more practical solution for simulations using modest computing powers (in this case, a 64 bit, 32 GB RAM and 3.7 GHz personal computer specification). The +FLOW solver in SIMPLEWARE avoids the use of quadratic elements for the velocity, making computation faster, using less memory [27]. For this reason, it was used to quantify the tradeoff between mesh element number and accuracy, when measuring the permeability using the highly refined HQTM mesh [16,27] and several different LTM mesh structures for subsequent use in COMSOL.

An optimization study was used to minimize modeling uncertainty and was performed on an RVE with 2 mm diameter spheres and a void fraction of 0.43. This approach has been proven successful to ensure accurate simulation of flow through inverse structures [24,28,29]. The optimization process varied the minimum and maximum edge lengths in multiples of the resolution of the original 2D images (voxel length = 21 μm). The growth rate had been optimized in an earlier study and was kept constant at 1.3. Figure 4 shows the difference in mesh geometry for structures having equal maximum edge length (3× the voxel dimension) and minimum edge lengths of 1× and 2.5× the voxel dimension. Table 1 presents a summary of the main findings, showing the change in the permeability ratio (the computed permeability to the benchmark obtained from the HQTM mesh) as a function of mesh geometry and the computational time for the solution. A sensible balance of computational efficiency and accuracy was identified (being mindful of the need to reduce the element count to below 3×10^6 cells for ease of use in COMSOL) by minimum and maximum edge lengths 2.5× and 3× the resolution, respectively, (shown in Fig. 4, right). For a mesh with 2.2×10^6 cells, the permeability is 96.9% of that for the HQTM mesh (6.155×10^{-9} m^2).

The optimized LTM mesh structure was exported to COMSOL MULTIPHYSICS 5.2 to solve the pressure drop in the Z-direction as a function of flow velocity. Flow was solved using the incompressible Navier–Stokes equation, with zero pressure outlet, no-slip walls (the same as imposed in SIMPLEWARE), and symmetrical boundary conditions on the side faces.

3 Simulation Using COMSOL

The pressure drop developed across packed bed structures containing 1, 2, and 3 mm diameter spheres, with different void fractions, was simulated for a range of water flow velocities between 0 and 0.1 m s^{-1} and is shown in Fig. 5. As expected, the pressure drop increases with increasing velocity and decreases with increasing porosity. Over the full range of velocities explored, the dependence between pressure drop per unit length and velocity could be accurately related ($R^2 = 1$) using a second-order polynomial, following the Forchheimer relationship presented in Eq. (3).

The transition from creeping (Darcy) flow to the onset of inertial (Forchheimer) flow can be determined by plotting the reduced

Table 1 Data for the mesh study using $L_{max} = 3\times$ resolution, varying L_{min}

L_{min} (mm)	Permeability/10^{-9}m^2	Mesh density/10^6	Permeability ratio	Growth rate	Homogenization time (s)
2.5×	5.95	2.190	0.967	1.30	346
2.0×	5.96	2.288	0.968	1.30	395
1.5×	5.96	2.764	0.968	1.30	469
1.0×	5.97	2.967	0.969	1.30	555

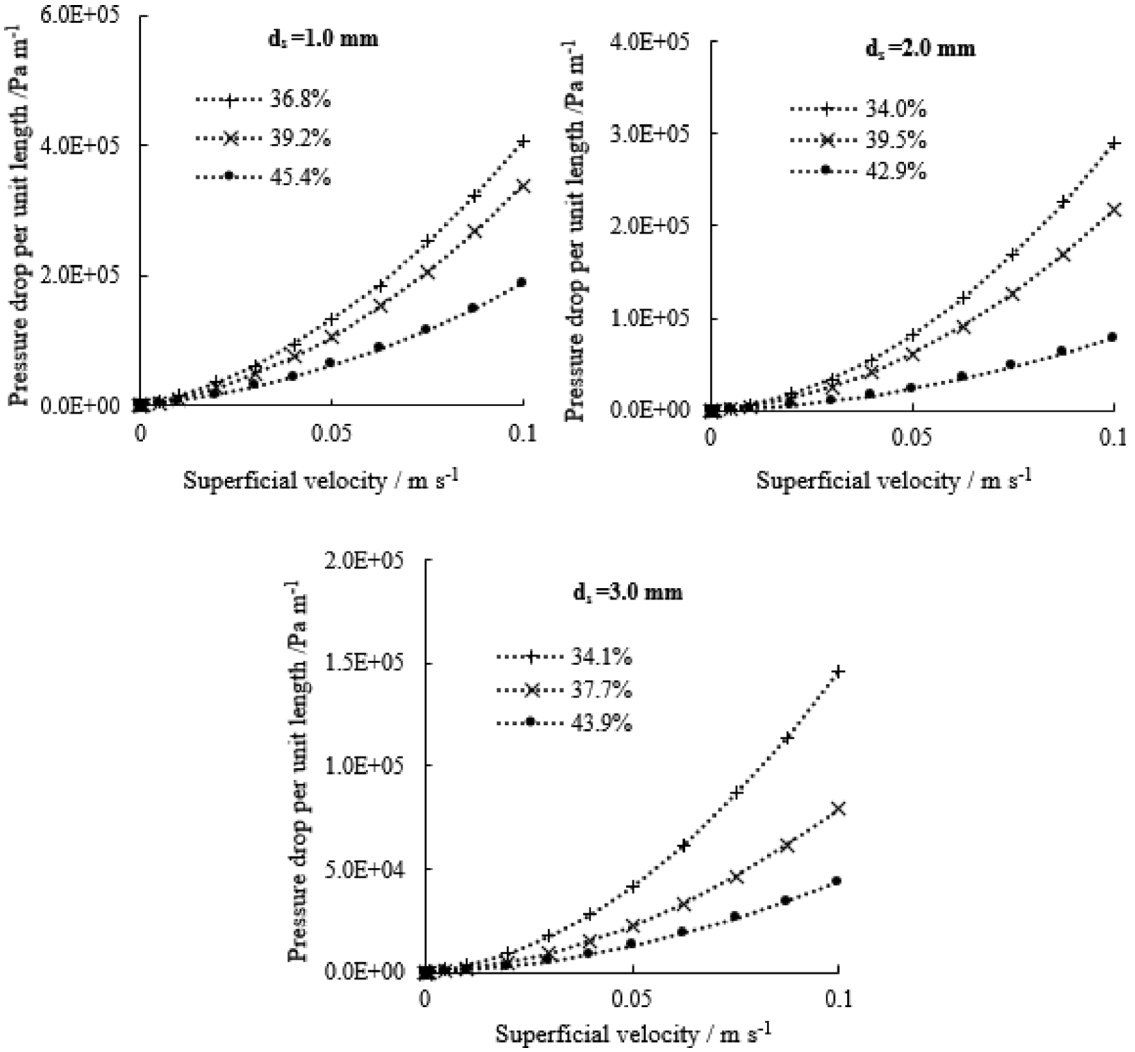

Fig. 5 Plots of pressure drop per unit flow length against superficial velocity, for 1, 2, and 3 mm spheres packed at different void percentages

pressure drop per unit length (the pressure drop per unit length divided by the flow velocity) against the flow velocity. The transition is identified by the change from a constant reduced velocity (Darcy regime) to one with linear dependency on velocity (Forchheimer regime). Figure 6 shows such plots for different sized spheres and void contents, showing both the full velocity range and isolating the low-velocity range. At higher superficial fluid velocities, the linear relationship is clear and at low velocities, typically below 1×10^{-4} m s^{-1}, the reduced pressure drop is independent of velocity and flow can be said to be in the Darcy regime. The exact value for the transition velocity did vary a little with sphere size and void fraction, increasing with decreasing sphere size and increasing void fraction. As was reported in Refs. [16,19,24,27], and [30], Darcy flow was observed for a pore-based Reynolds number (determined using Eq. (7)) less than unity.

$$\mathrm{Re} = \frac{\rho V d_s}{\mu} \tag{7}$$

Reduced pressure plots were also used to determine the permeability, k, from the pressure drop value for the plateau at low velocities, and the form drag term C, from the gradient of the linear section at higher velocities (using a water dynamic viscosity of 9.77×10^{-4} Pa·s and density of 998 kg m^{-3}). This approach was preferred to using values from the second-order polynomial fit to the curves, such as in Fig. 5 since fitting to the data points at higher velocities can result in significant errors to the fitting of points at very low velocities. The values obtained for these parameters are presented in Table 2.

In all instances, the permeability measured from COMSOL simulations over multiple flow velocities (at least six in the Darcy

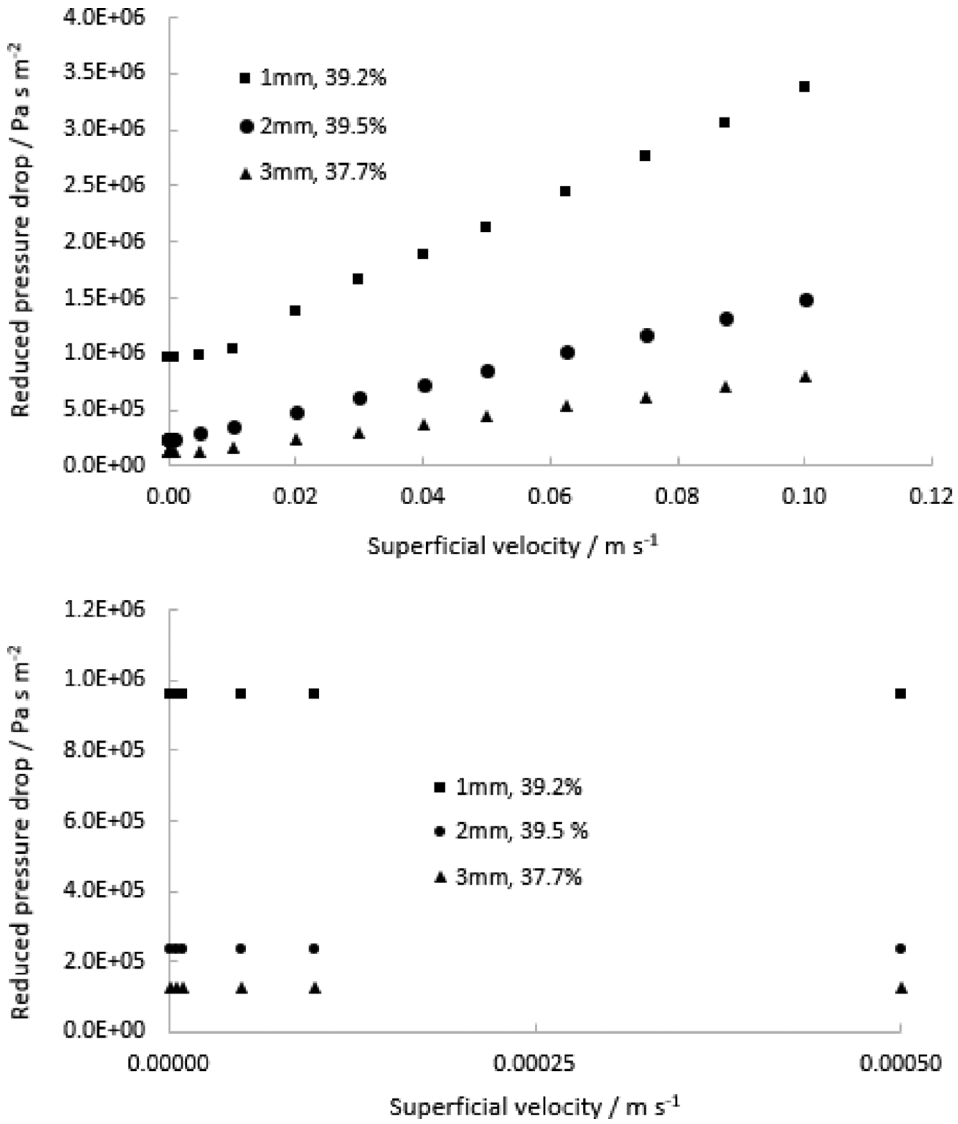

Fig. 6 Plots of reduced pressure drop against superficial fluid velocity for different spheres and void fractions (top: full velocity range, bottom: low velocity range)

Table 2 A comparison of the simulated flow parameters

d_s (mm)	(ε)	SIMPLEWARE $K/10^{-9}$m^2 (LTM mesh) Darcy regime	SIMPLEWARE $K/10^{-9}$m^2 (HQTM mesh) Darcy regime	COMSOL $k/10^{-9}$m^2 (LTM mesh)	COMSOL C (m^{-1}) (LTM mesh)
	0.368	0.770	0.796	0.775	27,359
1.0	0.392	0.998	1.032	1.016	23,988
	0.454	1.925	1.990	1.957	14,114
	0.340	2.218	2.293	2.256	22,546
2.0	0.395	4.125	4.265	4.203	12,543
	0.429	5.953	6.155	6.001	6329
	0.341	5.066	5.238	5.151	12,774
3.0	0.377	7.601	7.859	7.744	6568
	0.439	14.823	15.326	15.072	3753

regime) yields values that are intermediate between those for the highly refined and coarse mesh for single velocity measurement using the FLOW module in SIMPLEWARE. On average, they are 2% lower than the value for the finest (HQTM) mesh. This good agreement gives confidence in the robustness of the modeling approach, credibility to the convenience of using SIMPLEWARE to determine flow behavior in the Darcy regime, and justification of the use of coarser meshes within COMSOL as a practical approach to solving for multiple flow velocities.

The trends in modeled pressure drop in Fig. 5 are clear. As expected, pressure drops decrease not only with decreasing flow velocity but also with increasing void fraction and increasing particle size. Figure 7 shows typical 2D YZ sections of 3D velocity streamline plots for a pore inlet velocity in the Forchheimer

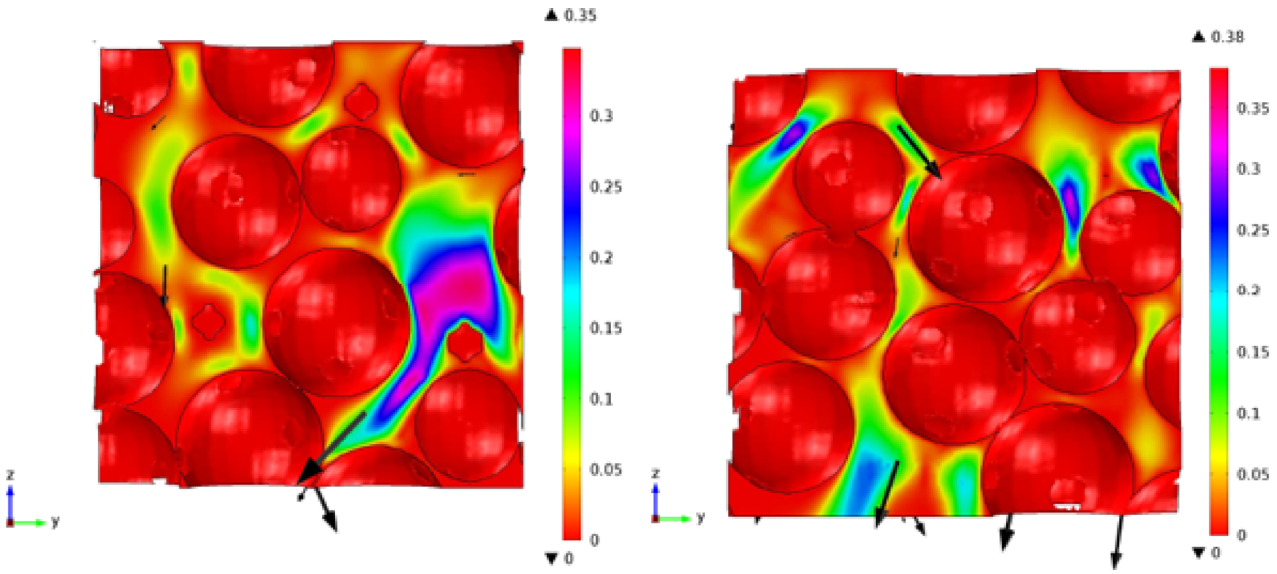

Fig. 7 Two-dimensional YZ sections from 3D images showing velocity streamlines for (left) 1.0 mm spheres, $\varepsilon = 0.368$, cube height = 3 mm and (right) 3.0 mm spheres, $\varepsilon = 0.341$, cube height = 9 mm. The pore inlet velocity in both cases is 0.05 m s^{-1} and the maxima on the velocity axes are 0.35 m s^{-1} and 0.38 m s^{-1}, respectively.

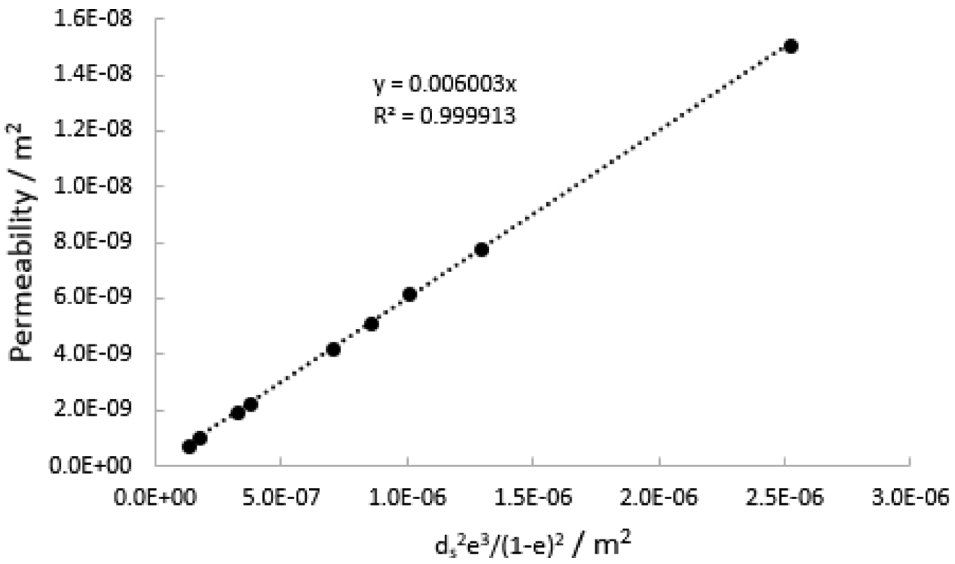

Fig. 8 Plot of CFD modeled permeability against structural parameters

regime (0.05 m s^{-1}). Localized regions with high flow velocity are clear in both images, caused by fluid flow through constrictions in the packed sphere structure.

4 Comparison With Analytical Models

By plotting the permeability against $d_s^2\varepsilon^3/(1-\varepsilon)^2$, it is clear from Eq. (2) that the slope yields $1/B_K$ from which the Kozeny constant, $B_K/36$, can be determined. Figure 8 presents such a plot, showing a near perfect fit to a straight line. From this, K was determined to be 4.64 ($B_K = 167$). This compares with values of 4.72 ($B_K = 170$) and 4.56 ($B_K = 164$) for permeability simulations using the LTM and HQTM meshes in SIMPLEWARE, respectively, and sits within the range of values reported for spherical beads (4.5–5.1) [2]. Analysis of individual data points showed B_K (or α as in the case of the Ergun relation in Eq. (4)) to vary very little around the average value, as the excellent fit suggests, with a standard deviation <1%. Such a tight distribution of values indicates little to no influence of other structural parameters on α for these packed beds.

Figure 9 shows a plot of C against $(1-\varepsilon)/(\varepsilon^3 d_s)$, from which the slope yields β, with a value of 2.35. Individual analysis of the inertial coefficient showed a large variation from 1.73 to 2.74 (a standard deviation of 16%), which is in keeping with the range reported in the literature [11–13,19,21]. There is an acceptance that C (in Eq. (3)) and therefore β will not be constant for a given structure for all flow velocities and many approaches (as appraised in Ref. [31]) suggest a constant value for $10 < \mathrm{Re} < 80$. Reappraisal of the data, using only superficial velocities corresponding to these limits, yielded some small changes in $\beta(\pm 2\%)$, but no significant reduction in the scatter. No clear dependence could be found for β upon simple structural parameters such as porosity, particle size, or surface area per unit volume. There was a tendency, however, for low β values for samples with low form drag coefficients, C, those structures at the upper range of porosity and particle size.

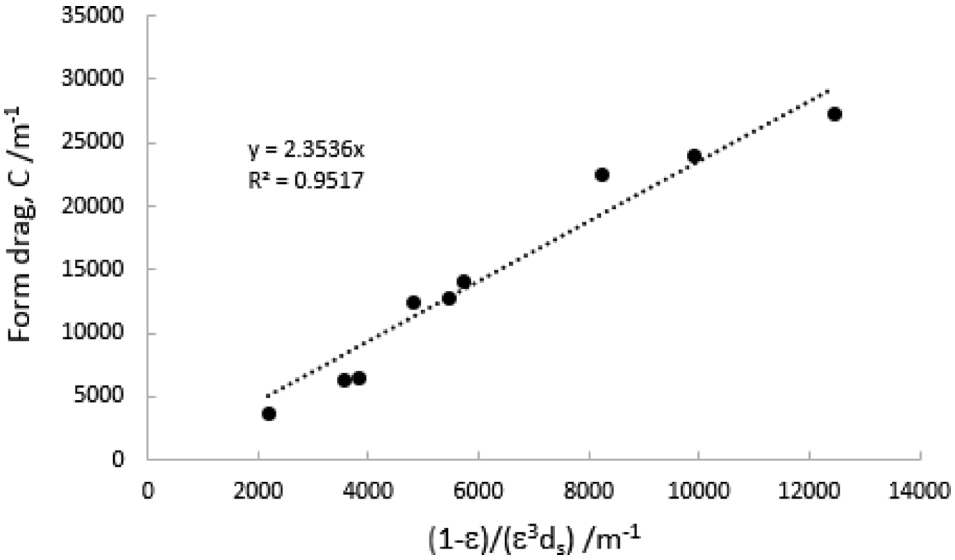

Fig. 9 Plots of CFD modeled form drag coefficient against structural parameters

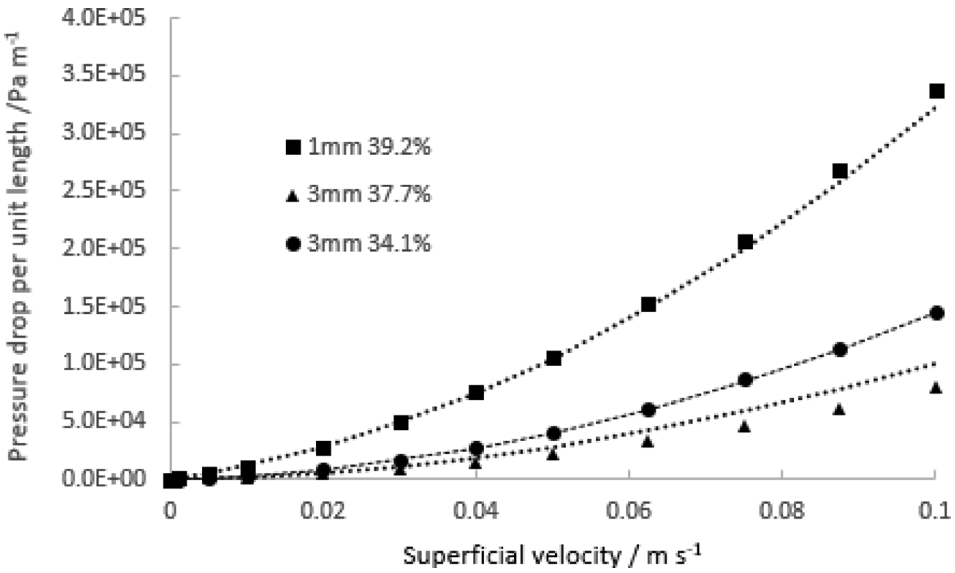

Fig. 10 Plots of CFD modeled permeability (solid symbols) compared with Eq. (4) (dashed lines)

Deviation from the average value for β for the structures investigated means that substitution back into the Ergun equation will have limitations on the accuracy of the prediction of pressure drop. Such an analysis is shown in Fig. 10 and is compared for selected samples that were presented earlier in Fig. 5. Predictions are accurate at low velocities owing to minimal scatter in the α term and because of the minimal influence of the inertial term. At higher velocities, the magnitude of the deviation depends upon the difference in α from the average (2.35). Examples are shown for samples with 1 mm diameter spheres (where $\beta = 2.42$) and 3 mm diameter spheres with lower porosity (where $\beta = 2.32$) and in both cases, the fit is very good. For the sample with 3 mm diameter spheres and higher porosity, ($\beta = 1.73$) there is as much as a 30% difference between values predicted by the Ergun equation and CFD modeling.

Despite using spherical particles for the simulation with identical size, roughness, and sphericity, significant variability in the Ergun coefficient, β, has been observed. The findings in this study bring strong support to the belief that a generalized model, such as that by Ergun [2–4], cannot yield a unique value for these constants, even for the case for spherical particles and laminar flow conditions [32]. This variation cannot be easily rationalized in terms of simple structural features and is most likely influenced by effects related to macroscopic variations in the packing arrangement (which, in this study, was random to replicate effects observed in experiments).

Figure 11 gives some additional insight into this effect, where 2D sections are presented that show velocity profiles and pressure distributions. At low porosity, packing is close to the upper limit for random packing of frictionless monosized spheres, with a high coordination number (measured in the MATLAB™ simulation to be 6.5) and a tight distribution of nearest neighbor distances. Such structures are likely to have very few packing defects, presenting similar pathways to the percolating fluid. Figure 11 (top) supports this, showing flow to be fairly evenly dispersed throughout the porous structure. At high porosity, close to the lower limit

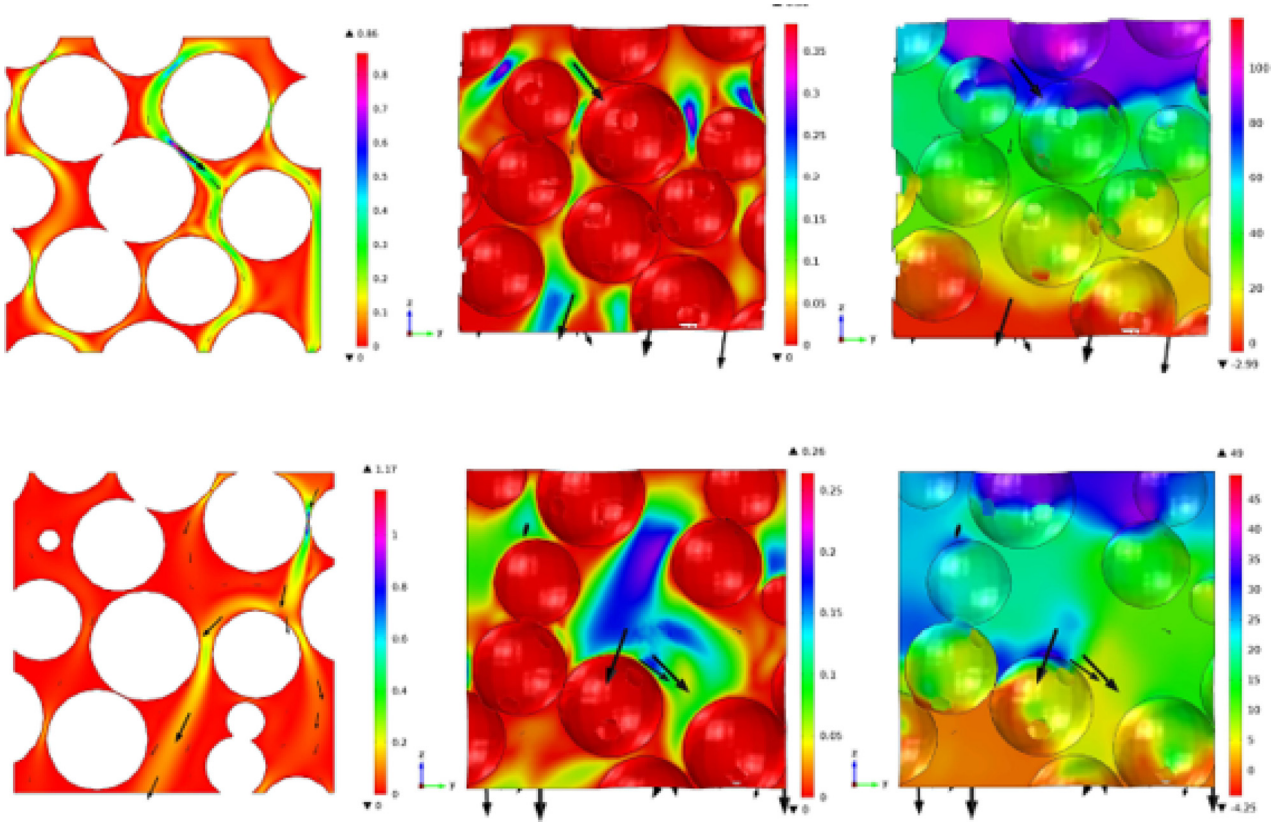

Fig. 11 Two-dimensional images of the velocity streamlines (left and center) and pressure plots (right) for 3.0 mm spheres, (top) $\varepsilon = 0.341$, (bottom) $\varepsilon = 0.439$. The pore inlet velocity in both cases is 0.05 m s^{-1} and the units on the velocity axes are in m s^{-1} and the pressure axes in MPa.

for loose packing of monosized spheres, the coordination number decreases to 3.5 and the distribution of nearest neighbor distances increases significantly. Figure 11 (bottom) shows that for this structure, flow is more highly localized through disproportionately large channels created by irregular packing. This preferential flow leads to lower form drag and a reduction in the value of β determined from this, an effect that is exacerbated by large particles, which result in larger channels.

5 Conclusions

Novel methods combining DEM simulations of packing and CFD modeling of fluid flow were used to simulate the pressure drop across rigid, randomly packed beds of spheres. This analysis was used to give insight into the ability of the well-established Ergun equation to predict such behavior.

Simulations yielded average values for α and β in the Ergun equation, of 167 and 2.35, respectively, for spheres ranging from 1 to 3 mm in diameter and void fractions from 0.34 to 0.45. The findings are in keeping with those reported in the literature.

While the scatter in α was small, the variation in β with structural parameters such as void fraction and particle size was large. Using an average value for β was found to lead to inaccuracies when predicting the pressure drop, particularly at higher velocities when the inertial term is dominant.

Although no clear relationship between β and simple structural parameters could be established, evaluation of the packed particle structures showed that areas of poor packing, in samples with high porosity and large particle sizes, lead to lower β values.

The findings in this study bring strong support to the belief that, owing to the effects imposed by macroscopic variations in the packing arrangement, a simple assumption of a generalized model, such as that by Ergun, cannot yield a unique value for β even for identical spheres.

Acknowledgment

OAJ would like to acknowledge the University of Nottingham for the receipt of a Dean's Scholarship.

References

[1] Muskat, M., and Botset, H. G., 1931, "Flow of Gas Through Porous Materials," Physics **1**(1), pp. 27–47.

[2] Harker, J. H., Richardson, J. F., and Backhurst, J. R., 2002, *Chemical Engineering*, Vol. 2, Elsevier Science and Technology, Oxford, UK.

[3] Ergun, S., 1952, "Fluid Flow Through Packed Columns," Chem. Eng. Prog., **48**, pp. 89–94.

[4] Carman, P. C., 1956, "Fluid Flow Through Granular Beds," Chem. Eng. Res. Des: Trans. Inst. Chem. Eng., Part A, **15**, pp. 415–421.

[5] Rahil, O., Tadrist, L., Miscevic, M., and Santini, R., 1997, "Fluid Flow Through Randomly Packed Monodisperse Fibers: The Kozeny-Carman Parameter Analysis," ASME J. Fluids Eng., **119**(1), pp. 188–192.

[6] Montillet, A., 2004, "Flow Through a Finite Packed Beds of Sphere: A Note on the Limit of Applicability of the Forchheimer-Type Equation," ASME J. Fluids Eng., **126**(1), pp. 139–143.

[7] Eisenklam, P., 1956, "Porous Masses," *Chemical Engineering Practise*, H. W. Cremer and T. Davies, eds., Vol. 2, Butterworths, London, pp. 342–463.

[8] Heijs, A. W. J., and Lowe, C. P., 1995, "Numerical Evaluation of the Permeability and Kozeny Constant for Two Types of Porous Media," Phys. Rev., ESI, **51**(5), p. 4346.

[9] Karimian, S. A. M., and Straatman, A. G., 2008, "CFD Study of the Hydraulic & Thermal Behaviour of Spherical -Void-Phase Porous Materials," Int. J. Heat Fluid Flow, **29**, pp. 292–305.

[10] Fand, R. M., and Thinakaran, R., 1990, "The Influence of the Wall on Flow Through Pipes Packed With Spheres," ASME J. Fluids Eng., **112**(1), pp. 84–88.

[11] Macdonald, I. F., El-Sayed, M. S., Mow, K., and Dullien, F. A. L., 1979, "Flow Through Porous Media: The Ergun Equation Revisited," Ind. Eng. Chem. Fundam., **18**(3), pp. 199–208.

[12] Plessis, P. J. D., and Woudberg, S., 2008, "Pore-Scale Derivation of the Ergun Equation to Enhance Its Adaptability and Generalization," Chem. Eng. Sci., **63**, pp. 2576–2586.

[13] Dudgeon, C. R., 1966, "An Experimental Study of the Flow of Water Through Coarse Granular Media," Houille Blanche, **21**, p. 785.

[14] Allen, K. G., von Backström, T. W., and Kröger, D. G., 2013, "Packed Bed Pressure Dependence on Particle Shape, Size Distribution, Packing Arrangement and Roughness," Powder Technol., **246**, pp. 590–600.
[15] Kays, W. M., and London, A. L., 1984, *Compact Heat Exchangers*, 3rd ed., McGraw-Hill, New York.
[16] Carter, T. J., Tanner, C., and Hawkes, D. J., 2015, "A Comparison of Linear and Quadratic Tetrahedral Finite Elements for Image-Guided Surgery Application," Centre for Medical Image Computing, University College London, London.
[17] Lage, J. L., Krueger, P. S., and Narasimham, A., 2005, "Protocol for Measuring Permeability and Form Coefficient of Porous Media," Phys. Fluids, **17**, p. 088101.
[18] Li, S., Zhou, L., Yang, J., and Wang, Q., 2018, "Numerical Simulation of Flow and Heat Transfer in Structured Packed Beds With Smooth or Dimpled Spheres at Low Channels to Particle Diameter Ratio," Energies, **11**(4), p. 937.
[19] Gunjal, P. R., Ranade, V. V., and Chaudhari, R. V., 2005, "Computational Study of a Single-Phase Flow in Packed Beds of Spheres," AIChE J., **51**(2), pp. 365–378.
[20] Guo, X., and Dai, R., 2010, "Numerical Simulation of Flow and Heat Transfer in a Random Packed Bed," Particuology, **8**(3), pp. 293–299.
[21] Dorai, F., Teixeira, M. C., Rolland, M., Climent, E., Marcoux, M., and Wachs, A., 2015, « "Fully Resolved Simulations of the Flow Through a Packed Bed of Cylinders: Effect of Size Distribution," Chem. Eng. Sci., **129**, pp. 180–192.
[22] Langston, P., and Kennedy, A. R., 2014, "Discrete Element Modelling of the Packing of Spheres & its Application to the Structure of Porous Metals Made by Infiltration of Packed Beds of NaCl Beads," Powder Technol., **268**, pp. 210–218.
[23] Otaru, A. J., and Kennedy, A. R., 2016, "The Permeability of Virtual Macroporous Structures Generated by Sphere Packing Models: Comparison With Analytical Models," Scr. Mater., **124**, pp. 30–33.
[24] Otaru, A. J., 2018, "Fluid Flow and Acoustic Absorption in Porous Metallic Structures Using Numerical Simulation and Experimentation," Ph.D. thesis, The University of Nottingham, Nottingham, UK.
[25] Otaru, A. J., Morvan, H. P., and Kennedy, A. R., 2018, "Measurement and Simulation of Pressure Drop Across Replicated Microcellular Aluminium in the Darcy-Forchheimer Regime," Acta Mater., **149**, pp. 265–275.
[26] Otaru, A. J., Morvan, H. P., and Kennedy, A. R., 2018, "Modelling and Optimisation of Sound Absorption in Replicated Microcellular Metals," Scr. Mater., **150**, pp. 152–155.
[27] Schneiders, R., 2000, "Octree-Based Hexahedral Mesh Generation," Int. J. Comput. Geom. Appl., **10**(04), pp. 383–398.
[28] Otaru, A. J., 2019, "Enhancing the Sound Absorption Performance of Porous Metals Using Tomography Images," Appl. Acoust., **143**, pp. 183–189.
[29] Duggirala, R. K., Roy, C. J., Saeidi, S. M., Khodadadi, J. M., Cahela, D. R., and Tatarchuk, B. J., 2008, "Pressure Drop Predictions in Microfibrous Materials Using Computational Fluid Dynamics," ASME J. Fluids Eng., **130**(7), pp. 1–13.
[30] Otaru, A. J., Morvan, H. P., and Kennedy, A. R., 2019, "Airflow Measurement Across Negatively Infiltration Processed Porous Aluminium Structures," AIChE J. (epub).
[31] Sidiropoulou, M. G., Moutsopoulos, K. N., and Tsihrintzis, V. A., 2007, "Determination of Forchheimer Equation Coefficients a and b," Hydrol. Process, **21**(4), pp. 534–554.
[32] Ozahi, E. O., Gundogdu, M. Y., and Carpinlioglu, M. O., 2007, "A Modification on Ergun's Correlation for Use in Cylindrical Packed Beds With Non-Spherical Particles," Adv. Powder Technol., **19**(4), pp. 369–381.